

Multi-Step toolpath approach to overcome forming limitations in single point incremental forming

J. Verbert¹, B. Belkassem², C. Henrard³,
A.M. Habraken³, J. Gu², H. Sol², B. Lauwers¹, J.R. Duflou¹

¹Katholieke Universiteit Leuven – Department of Mechanical Engineering - Leuven
URL: www.kuleuven.be e-mail: Johan.Verbert@mech.kuleuven.be;

²Vrije Universiteit Brussel - Vakgroep Mechanica van Materialen en Constructies – Brussels
URL: www.vub.ac.be e-mail: Bachir.Belkassem@vub.ac.be;

³Université de Liège - Département M&S Mécanique des matériaux et Structures - Liège
URL: www.ulg.ac.be e-mail: Christophe.Henrard@ulg.ac.be;

ABSTRACT: Although Incremental Forming offers distinct advantages over traditional forming processes, such as short lead times and low setup costs, the process still has some drawbacks. Besides the obtainable accuracy, one of the main challenges of the process are the process limits. Many workpiece geometries cannot be manufactured due to the fact that the maximum wall angle that can be formed is limited for a certain sheet material and thickness to a given angle. Different solutions to this approach have been proposed and this paper further investigates one of those solutions, the multi step approach for single point incremental forming. Experiments were performed and compared with simulations to better understand the phenomena underlying the improved process performance.

Key words: SPIF, Incremental forming, Process limits.

1 INTRODUCTION

Single Point Incremental Forming (SPIF) is a sheet metal part production technique by which a sheet metal part is formed in a stepwise fashion by a CNC controlled spherical tool without the need for any supporting die. This technique allows a fast and cheap production of customized or small series of sheet metal parts [1].

Besides the obtainable accuracy [2], one of the main challenges of the process are the process limits. Many workpiece geometries cannot be manufactured due to the fact that the maximum wall angle that can be formed is limited for a certain sheet material and thickness to a given angle α (see Figure 1) [3]. If a sufficiently large portion of a workpiece has a wall angle that exceeds this angle, the part will fail during manufacturing.

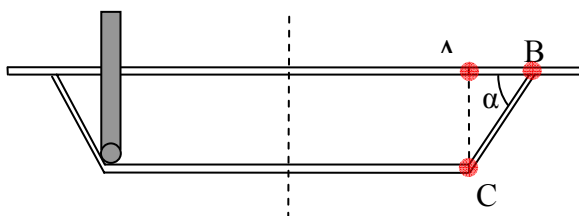


Fig. 1: Sectional view of a cone

2 THEORETICAL BACKGROUND AND OBJECTIVE

The process limits of SPIF can be intuitively explained intuitively by the sine law. The zone of material AB in the original flat sheet (see Figure 1) will be stretched into the zone CB of the final part during the forming process.

$$T_{CB} = T_{AB} \sin(90 - \alpha)$$

Formula 1: Sine law

Assuming that only in-plane strains occur, the sine law can be used to estimate the final thickness of the part at zone CB (T_{CB}) from the original thickness of the zone AB (T_{AB}) and the wall angle of the part (α). It has experimentally been verified that the process more or less follows this law [4] with a tendency to overform slightly [5].

In Table 1 a set of maximum wall angles for commonly used materials is given as a function of the thickness of the sheet and the diameter of the tool used during forming. As can be seen from the table, parts with (semi-) vertical walls are impossible to form using standard milling toolpaths as generated by most CAD/CAM packages.

Material	Thickness (mm)	Tool Ø (mm)	Max. wall angle
Al 3003-O	1.2	10	71°
Al 3003-O	2.0	10	76°
AA 3103	0.85	10	71°
AA 3103	1.5	10	75°
Ti Grade 2	0.5	10	47°
DC01	1.0	10	67°
AISI 304	0.4	10	63°

Table 1: Common materials with their failure angles

From the sine law formula it follows that the steeper the wall angle, the greater the thinning of the zone CB. In order to increase the maximum wall angle, one could increase the starting thickness (T_{AB}) of the sheet, as can be seen in the experiments reported in Table 1. This strategy has its limitations due to maximum machine load and overall part thickness specifications. Finally, the only way to obtain large wall angles is to aim for material redistribution by shifting material from other zones in the part to the inclined wall areas.

Several authors have already reported on multi-pass forming. Consecutive toolpaths, corresponding to virtual parts with increasing wall angles, are being executed in a multi-step procedure. [5][6][7]. The aim of this paper is to further investigate the mechanics behind the multi-step forming approach to contribute to a better understanding of the material relocation mechanism underlying the enlarged process window.

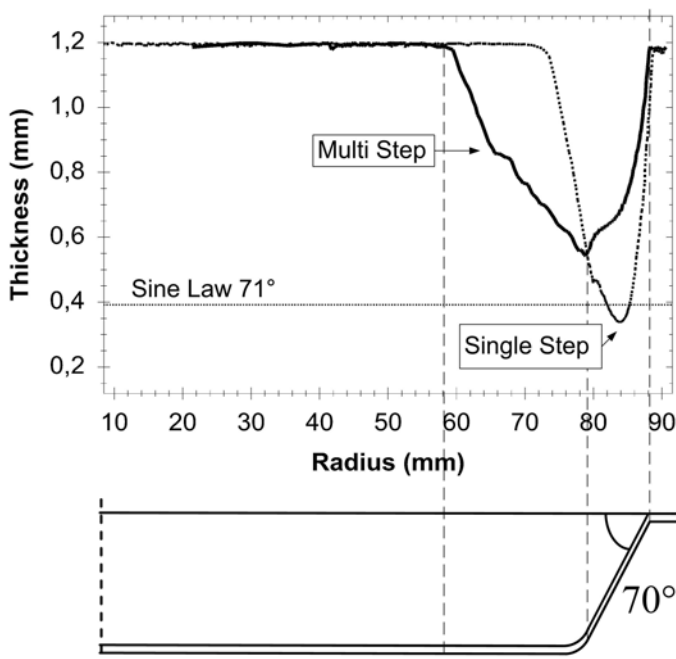


Fig. 2: Geometry and thickness in function of radius

3 EXPERIMENTAL EXPLORATION

3.1 Experimental Setup

The experiments were performed on a three-axis milling machine with a horizontal spindle. This allowed in-process observation of the part being formed by means of a stereo camera setup and Digital Image Correlation (DIC).

For each of the tests, a spherical tool with a diameter of 10mm was chosen with the feedrate set to 2m/min and the spindle speed fixed at 100 rotations/min. Oil was used as lubricant. The setup allowed to remove the part within its clamping rig from the machine without unclamping the part itself, allowing the part to remain clamped during consecutive manufacturing and measuring steps.

3.2 Comparison of the thickness distribution for single and multi-step formed parts

For the first set of experiments, two cones with a 70 degree wall angle were manufactured. Both cones have an upper inner diameter of 178mm and a internal depth of 30mm. The diameter of the backing plate was 182mm. A single-step reference part was compared with a part formed with two intermediate steps at 50° and 60°. The sheet material was Al3003-O with a thickness of 1.2mm.

In Figure 2 the thickness profiles of both cones are plotted in function of the radius. As can be seen, the wall thickness of the multi-step cone is significantly larger than the thickness obtained with the single-step toolpath. However, the thickness of the bottom of the multi-step part is lower than the thickness of the bottom of the single-step part. Using the multi-step approach has clearly led to a shift of material from the bottom, which would otherwise have remained unprocessed, to the wall of the part.

3.3 Forming of a cylindrical part in 5 steps

3.3.a Test setup

Aim of this experiment was to quantify the material flow during consecutive steps of forming. A cone was manufactured in 5 passes with a 10° increase in the wall angle between each step, starting from 50°. The sheet material used for these tests was AA3103 with a thickness of 1.5mm. The workpiece had an upper diameter of 128mm and a programmed depth of 30mm. The diameter of the backing plate was 131mm, close to the part to eliminate most of the bending that is induced by multi-step forming. A 10mm diameter tool and a contouring toolpath were used with a stepdown of 1mm per contour.

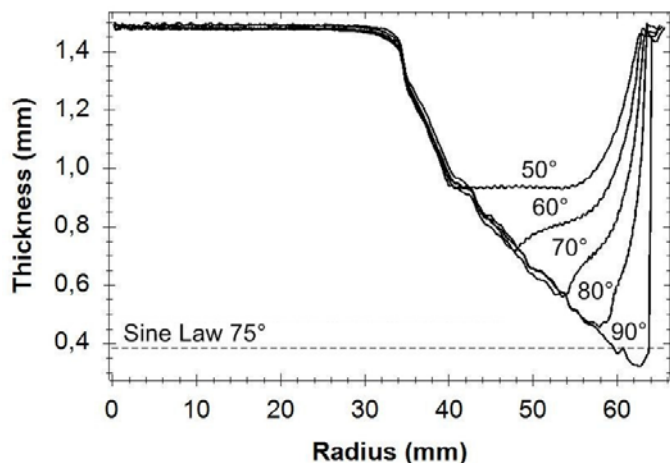


Fig. 3: Thickness in function of radial dimension

3.3.b Experimental results

In Figure 3 the measured thickness profiles of the cones in the different steps and the theoretical sine law thickness are plotted against the radial dimension. As can be seen, the thickness profile of the first step (50°) determines the thickness profiles of the following steps. The part was close to failure near the bottom since the thickness of the 90° part is, at its thinnest point, lower than the failure thickness as predicted by the sine law for 75°.

3.3.c Digital Image Correlation results

To be able to track the material flow during the process, the outer surface of the cone was measured during forming with a Limes stereo camera setup. After processing this data with a Digital Image Correlation system (DIC), 36 points from the outer surface of the cone, defining a planar section of the outer surface, were selected and tracked during the forming process (see Figure 4). The thick curves represent the shape of the part at the end of each of the five consecutive forming steps. The thin curves visualise the trajectories of each of the observed points on the outer surface based on 2030 intermediate observations.

As can be seen in Figure 4, the sine law is an acceptable approximation for the first step of the multi step approach: when forming the first, 50° cone, the points are translated quasi downwards. This corresponds to a very limited tangential strain. For the next steps, however, the sine law is no longer valid. Instead of a downward translation, the points are quasi rotated about the backing plate edge. The closer to the bottom of the part, the larger the horizontal distance between two consecutive step sections becomes and the more the rotational motion transforms into a downward translation. In contrast with single-step forming, where maximum thinning and failure typically occur 10 to 15mm below the backing plate level, the edge of the cone bottom is also the location where failure can be expected to occur first in a multi-step strategy.

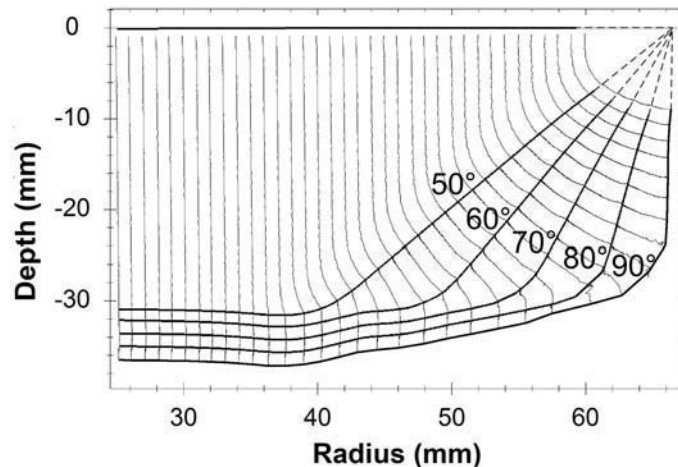


Fig. 4: DIC results

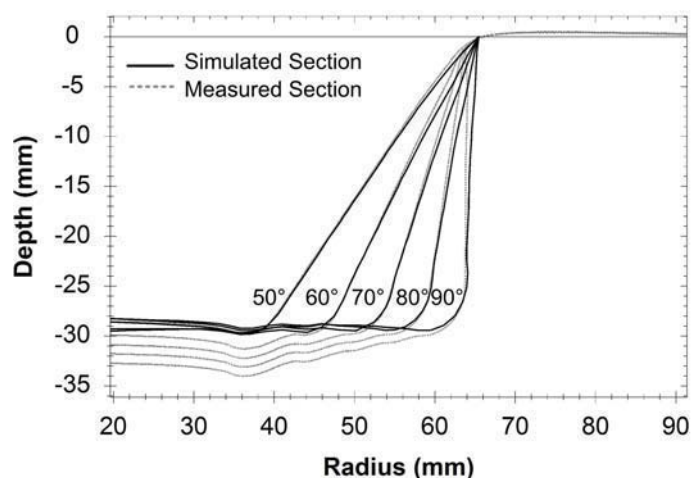


Fig. 5: Simulated and measured profiles

3.3.d FE Simulation

The same experiments were also simulated using Lagamine, a finite element code developed at the University of Liège [8]. The implicit time integration scheme was chosen here in combination with a second order shell element (COQJ4) [9]. The test part was modelled as a 45-degree segment with symmetry imposing boundary conditions at the edges. Even though the process itself is not rotationally symmetric, this approximation was found to provide useful results in the middle of the pie segment. The material model used was a Hill law with Swift-type isotropic hardening, for which the parameters were determined by means of a tensile and a Bauschinger shear test. The elastic parameters are $E = 72600$ MPa and $\nu = 0.36$. The yield locus is described using the Hill 1948 law with $F = 1.2241$, $G = 1.1933$, $H = 0.8067$ and $N = 4.060$.

$$\sigma_F = K(\epsilon_0 + \epsilon^p)^n$$

Formula 2: Swift Law

The hardening law is given by the Swift law (see Formula 2) with the following material parameters: $K = 183$ MPa, $\epsilon_0 = 0.00057$ and $n = 0.229$.

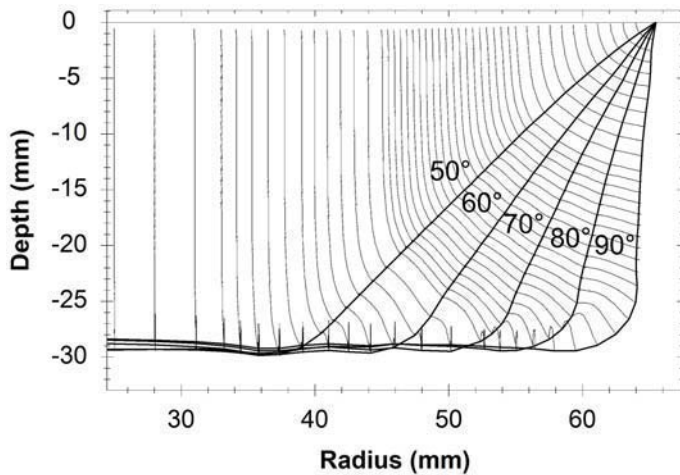


Fig. 6: Simulated material flow

Figure 5 illustrates that the bottom of the workpiece is not as accurately predicted as the wall. The symmetry imposing boundary conditions introduce an error. It has already been shown in a previous article [10] that the bottom of a single-step cone could be predicted more accurately if the whole part was modelled. This deviation seems to accumulate when simulating a multi-step toolpath. The obtained wall geometry, the material flow (see Figure 6) and the simulated strains however correspond well with the experimentally obtained results.

4 CASE STUDIES

A method for automatic multi-step toolpath generation was developed and successfully tested in a number of case studies. The part in Figure 7, a mould for composite pressure vessel production, has a vertical wall of 30 mm on top of which a hemisphere is modelled. Figure 8 illustrates that also for non-rotative geometries the multi-step approach remains applicable. The limits for achievable minimum radii between vertical walls are object of further research. Figure 9 shows an implant manufactured in 0.7 mm grade 2 titanium. A multi-step toolpath made it possible to form angles up to 61° while respecting the thickness requirements.

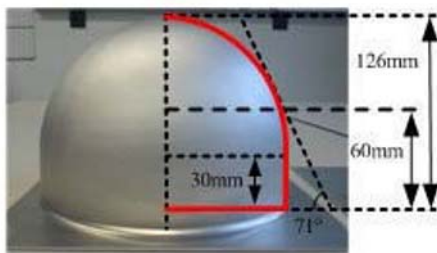


Fig. 7: Composite pressure vessel mould

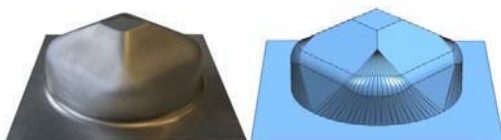


Fig. 8: Non-rotational part

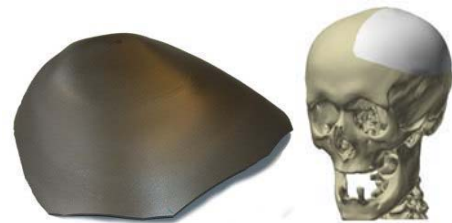


Fig. 9: Titanium cranial implant
(right image courtesy of SimiCure)

5 CONCLUSIONS

The extended process window achievable by means of multi-step SPIF can be explained by the straining of (semi-) horizontal workpiece areas that remain unaffected in conventional toolpath strategies. This allows to produce vertical walls without leading to part failure. The resulting thinning of the sheet during multi-step forming can exceed the maximum thickness reductions observed in single-step processing, implying a formability shift. The research shows a shift from a sine law like behaviour for the first step of the process to a more bending like behaviour for the following steps.

REFERENCES

1. Jeswiet J., Micari F., Hirt G., Bramley A., Duflou J.R. and Allwood J., 2005, *Asymmetric single point incremental forming of sheet metal*, CIRP Annals - Manufacturing Technology, 54/2:623-649
2. Duflou J.R., Lauwers B., Verbert J., Tuncol Y., De Baerdemaeker H., 2005, *Achievable Accuracy in Single Point Incremental Forming: Case Studies*, Proc. of the 8th Esaform Conf. Vol. 2., pp. 675-678.
3. Ham M., Jeswiet J., 2007, *Forming Limit Curves in Single Point Incremental Forming*, CIRP Annals-Manufacturing. Technology, 56/1:277-280.
4. Matsubara S., 2001, *A computer numerically controlled dieless incremental forming of a sheet metal*, J. of Engineering Manufacture. 215/7:959-966
5. Young D. and Jeswiet J., 2004, *Wall thickness variations in single-point incremental forming*, J. of Engineering Manufacture, 18/11:1453-1459
6. Kim T.J., Yang D.Y., 2001, *Improvement of formability for the incremental sheet metal forming process*, Int. J. of Mech. Sciences, 42:1271-1286
7. Hirt G., Ames J., Bambach M. and Kopp R., 2003, *Forming strategies and Process Modelling for CNC Incremental Sheet Forming*, CIRP Annals - Manufacturing Technology, V53/1, pp 203-206
8. Cescotto S. and Grober H., 1985, *Calibration and Application of an Elastic-Visco-Plastic Constitutive Equation for Steels in Hot-Rolling conditions*, Engineering Computations, 2:101-106
9. Jetteur P. and Cescotto S., 1991, *A Mixed Finite Element for the Analysis of Large Inelastic Strains*, Int. J. for Numerical Methods in Eng., 31:229-239
10. He S., Van Bael A., Van Houtte P., Szekeres A., Duflou J.R., Henrard C. and Habraken A.M., 2005 *Finite Element Modeling of Incremental Forming of Aluminum Sheets*, Adv. Mat. Research, 6-8:525-532